Int. J. Electrochem. Sci., 16 **(2021)** Article ID: 210742, doi: 10.20964/2021.07.71

International Journal of
ELECTROCHEMICAL
SCIENCE
www.electrochemsci.org

The Microstructure and Properties of Nitrided Chromium Coating on 316 Stainless Steels Fabricated by Electrodeposition and Electrolytic Nitriding for PEMFC Bipolar Plate

Yaxue Wang[1], *Chengwei Deng*[2], *Yi Sun*[2], *Xixun Shen*[1,*], *and Yanyan Zhu*[1]

[1] Shanghai Key Laboratory of Materials Protection and Advanced Materials in Electric Power, Shanghai Engineering Research Center of Heat-exchange System and Energy Saving, College of Environmental and Chemical Engineering, Shanghai University of Electric Power, Shanghai 200090, China
[2] Space Power Technology State Key Laboratory, Shanghai Institute of Space Power-Sources,Shanghai 200245, China
[*]E-mail: shenxixun@shiep.edu.cn

Received: 29 March 2021 / *Accepted:* 18 May 2021 / *Published:* 31 May 2021

In this paper, a nitrited chromium composite coating is fabricated as a protective coating for the 316 stainless steels bipolar plates by a combination process of electrodeposition and liquid-phase plasma electrolysis. The pre-treatment of chemical micro etching on the stainless steel substrate is also done to improve the adhesion between the coating and the substrate before electroplating and give the coating a rough surface with micro-nano structure.The electrochemical analysis revealed that the composite coating remarkably improve the corrosion resistance of the 316 stainless steels bipolar plates. The corrosion current density of the nitrited chromium composite coating in the simulated cathodic environment of PEMFC is only less than 9.35×10^{-7} A/cm^2, which nearly is three orders of magnitude lower than that of stainless steels substrate. Moreover, the composite coating has good long-term stability in corrosion resistance.After a long time of immersion, the corrosion current density of the coating remains at the same level as that before immersion.The interface contact resistance value of nitrited chromium composite coating is 4.9m$\Omega\cdot$cm^2 under the pressure of 1.4MPa, which meets the conductivity requirements of the bipolar plate.

Keywords: Stainless steel bipolar plate; Etching; Nitriding; Corrosion resistance; Interface contact resistance

1. INTRODUCTION

Proton exchange membrane fuel cell (PEMFC) is a promising energy source, with the advantages of high power density, low operating temperature and environmental protection [1-3]. The bipolar plate is the main component of the PEMFC, accounting for 70% ~ 80% of the total weight of the battery and 45% of the cost. The function of the bipolar plate is to separate the gas, conduct the current, connect the single cell, and maintain the stable operation of the PEMFC [4]. The ideal bipolar plate material must have: electrical and thermal conductivity, gas barrier function, high mechanical strength, corrosion resistance and easy processing [5,6]. Graphite is a traditional bipolar plate material with good chemical stability [7], but its brittleness leads to processing difficulties and increases production costs [8,9]. In recent years, people are actively seeking new alternative materials, and stainless steel is a popular candidate material for bipolar plates [10]. Stainless steel has good electrical and thermal conductivity and chemical stability, high mechanical strength and gas barrier function, low cost, suitable for mass production [11,12]. Therefore, stainless steel is the material of choice for bipolar plates. However, stainless steel is prone to corrosion and passivation under the acidic conditions of PEMFC. The metal ions produced by the corrosion will contaminate the electrode and affect the service life of the battery. Passivation increases the contact resistance of the bipolar plate and reduces the conductivity of the battery [13, 14]. Therefore, improving the corrosion resistance and conductivity of stainless steel is a prerequisite for ensuring the commercial application of stainless steel bipolar plates.

Surface modification is the most feasible method to prevent corrosion and oxidation of stainless steel bipolar plates. In order to improve the conductivity and corrosion resistance of stainless steel, a large number of studies have been conducted on the surface modification coating of stainless steel at home and abroad. Stainless steel modified coatings mainly include rare precious metal coatings, metal oxide coatings, transition metal nitride coatings and conductive polymer coatings. Rare and precious metal coatings were the first to be used for surface modification of stainless steel due to their good chemical stability and electrical conductivity [15]. Rare precious metals mainly include gold, platinum, niobium, silver [16,17], The coating effectively improves the corrosion resistance and conductivity of the bipolar plate, but the high cost also limits its commercial application. Metal oxide coatings based on tin and lead [18] improve the corrosion resistance of stainless steel, but the electrical conductivity is not ideal. Therefore, the metal oxide coating cannot meet the requirements of the bipolar plate. Conductive polymer coatings represented by polyaniline and polypyrrole have also been applied to the surface protection of stainless steel.For example, Joseph [19] deposited polyaniline and polypyrrole on the surface of 304 stainless steel by cyclic voltammetry, which significantly improved the corrosion resistance, but the conductivity was low. Wang [20] and others added graphene nanoparticles to the polymer coating, and the corrosion resistance and conductivity of the graphene / polyaniline composite coating were significantly improved in the acidic environment of penfc. However, this method can improve the conductivity of the composite, but only compared with the polyaniline coating, compared with the metal substrate, its conductivity still can not meet the commercial needs of PEMFC. Compared with other coatings, transition metal nitride coatings based on Cr and Ti have better corrosion resistance and conductivity, so they are considered to be the best choice for bipolar plates. Lee [21] used PVD to deposit CrN coating on 316 stainless steel, the corrosion current density decreased significantly under

the simulated PEMFC working environment, and the interface contact resistance met the performance index set by the U.S. Department of energy. Brady [22] Prepared chromium nitride coating on the surface of stainless steel by arc ion plating, and the corrosion resistance and conductivity of the modified stainless steel bipolar plate were better optimized. More and more studies have confirmed that the CrN coating prepared on stainless steel by a similar physical vapor deposition method can effectively improve the corrosion resistance and conductivity of the bipolar plate. The coating prepared by this physical vapor deposition (PVD) usually has some defects, such as porosity, non compactness, easy peeling and furthermore the production cost is high[23,24]. Therefore, it is necessary to find other processes to prepare chromium based nitriding composite coating to improve the corrosion resistance and conductivity of stainless steel bipolar plate.

In this paper, a liquid-phase electrochemical method involving electrodeposition and electrochemical plasma nitriding is proposed to construct chromium based nitriding composite coatings on the stainless steel bipolar plates because of its simple operation, flexible process control and low preparation cost[25-28]. In this process, firstly, a layer of chromium coating was deposited on the surface of stainless steel substrate by electroplating process, and then an electrochemical plasma nitriding process was carried out to nitride the chromium coating.In addition, in order to improve the bonding strength between the coating and the substrate to ensure the stable operation of the stainless steel bipolar plate, a micro chemical etching process is also applied to the stainless steel bipolar plate substrate to construct a micro nano structure surface before electroplating, in order to improve the bonding strength between the coating and the substrate. The morphology, composition and crystal structure of the coating were characterized by SEM, EDS and XRD, and the influence of the surface structure of the coating on the hydrophobicity was analyzed. The corrosion resistance and conductivity of the nitrited chromium composite coating were studied.

2. EXPERIMENTAL

2.1. Preparation of nitrited chromium composite coating

A nitrited chromium composite coating is prepared on the surface of 316 stainless steel by electrodeposition and liquid-phase plasma electrolytic nitriding. First, the electrodeposition method is used to deposit the chromium layer on the surface of chemically etched 316 stainless steel from an electrolyte containing trivalent chromium on stainless steel surfaces, and subsequently the chromium layer is nitridated in a nitriding solution including 500mL formamide, 100g/L urea and 1g/L potassium chloride. Stainless steel samples with a size of 100 mm×10 mm×0.3 mm cut by an electric spark cutter as the cathode plate, and the treated graphite plate is used as the anode. Before electrdeposition, the samples of 316 stainless steel (20 mm×20 mm×3 mm) were polished with different specifications of sandpaper (models 500# to 2000#) to remove the rust layer, then soaked in 20% sodium hydroxide solution to remove the surface pollution, activated in 20% dilute hydrochloric acid solution for 10 s, and finally washed with deionized water for standby.The cleaned 316 stainless steel is immersed in a chemical etching solution composed of $FeCl_3$ and HCl at a concentration ratio of 1:1 for 25 minutes. The

composition of the chromium plating bath includes 105g/L $CrCl_3$, 37g/L $HCOONH_4$, 27g/L CH_3COONa, 80g/L NH_4Cl, 37g/L KCl, 9g/L NH_4Br, 40g/L H_3BO_3, 0.2g/L SDS. The deposition current density is 8-15A/dm^2, the bath temperature is controlled at 35℃ and the mechanical stirring is 300 rpm, the electrodeposition time can be flexibly controlled between 1-60min, and a chromium plating layer with controllable thickness can be obtained on the stainless steel bipolar plate. For the liquid-phase plasma electrolysis nitriding treatment, the chrome-plated 316 stainless steel acts as a cathode plate, and the degreased platinum plate as a anode plate. Set the nitriding voltage to 300V, the nitriding current to 10A/cm^2, and the reaction temperature is 0-20℃, after 10 minutes of electrolytic nitriding, a chromium nitride composite coating can be prepared on the surface of 316 stainless steel.

2.2. Characterization

The surface morphology of nitrited chromium composite coating was observed by field emission scanning electron microscopy (FE-SEM, JSM-7800F operated at 5 kV) and characterized by energy dispersive spectrometer (EDS). X-ray diffraction (XRD, Cu Kα radiation, Bruker, D8 Advance, Germany) was used to analyze the change of crystal structure,Use contact angle measuring instrument to measure contact angle.

The electrochemical workstation (CHI660) is used to conduct electrochemical tests on the test samples. The test solution is a simulated corrosion solution of 0.5M H_2SO_4 + 5ppm NaF at a constant temperature of 30°C, using a traditional three-electrode system, with a saturated calomel electrode and a platinum electrode as the reference electrode and counter electrode, and the sample to be tested is the working electrode. Before electrochemical measurement, oxygenate the acidic solution containing fluoride ions for 30 minutes to make the test system more stable. The sample to be tested is immersed in a saturated oxygen solution for 10 minutes, and the exposed area is constant at 4cm^2, and then the open circuit potential is measured for 400s. The sweep rate of the potential polarization curve is 2mV/s, and the sweep potential range is -0.6V~1.0V; the frequency range of electrochemical impedance spectroscopy is 0.01Hz-100kHz, and the 5mV AC excitation signal is selected and the open circuit voltage is used as the input voltage for analysis. The immersion test experiment is to immerse the sample in a 0.5M H_2SO_4 + 5ppm NaF solution in a PEMFC simulated environment for 1 hour, 3 days, and 7 days, and then conduct an electrochemical test.

The interface contact resistance test is to sandwich the sample between two pieces of conductive carbon paper, and then put it between two gold-plated copper plates. After applying different pressures, use the ZY9858 DC resistance measuring instrument to read the value and calculate it.

3. RESULTS AND DISCUSSION

3.1. Surface morphology

Unetched 316 stainless steel shown in figure (a) has a flat surface and a contact angle of only 75.94°. It can be seen from figure (b) that the etched 316 stainless steel has rough surface, and the overall

structure is strip and honeycomb, and the contact angle increases to 123.17°. The surface morphology of the chromium coating on the corroded 316 stainless steel is shown in Figure (c). The micro-nano structure on the surface is mainly composed of spherical nodules with a contact angle of 122.77°. Some literatures pointed out [29, 30] that the surface of Cr coating is prone to cracks, so that the coating loses its protective ability. In this report, there are no cracks on the coating surface, which eliminates the possibility of corrosive ions contacting the substrate. The surface morphology of nitrited chromium composite coating on etched 316 stainless steel is shown in Figure (d). It can be seen from the figure that after further nitriding, the coating surface has no obvious change and still maintains micro-nano structure, with a contact angle of 124.73°. In this study, the contact angle of unetched 316 stainless steel does not exceed 90°, it's a hydrophilic surface. The surface of the etched 316 stainless steel and its modified coating has a unique micro-nano structure, so that the contact angle exceeds 120°, Showing obvious hydrophobicity.

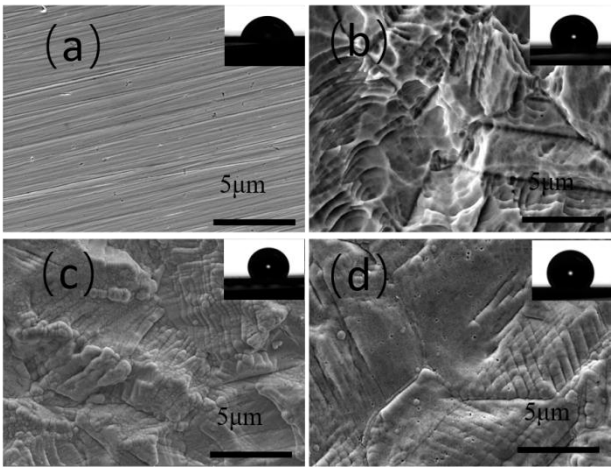

Figure 1. SEM surface morphology: (a) no etching of 316 stainless steel, (b) etching of 316 stainless steel, (c) Chromium coating on etched 316 stainless steel, (d) nitrited chromium composite coating on etched 316 stainless steel

3.2. Component analysis

The surface scan of nitrited chromium composite coating on etched 316 stainless steel is shown in Figure 2. It can be seen from Figure 2 that the coating is mainly composed of chromium and nitrogen, and the main element of the coating is chromium, and nitrogen is uniformly distributed in the chromium coating. Figure 3 is a line scan of a cross-section of a chromium nitrogen composite coating. It can be seen from Figure 3(a) that the overall nitrited chromium composite coating has a columnar structure with a deposition thickness of 24μm, the thickness of the coating can be adjusted by the reaction time. The coating is tightly combined with the substrate, this is not only the etching increases the surface roughness of the substrate, but also because the etching removes the interface oxide layer, which helps to improve the adhesion of the coating [31]. The linear scan direction of Figure 3(b) is from the substrate to the

coating. The main elements in the base material are Fe and Ni. After the scanning area enters the coating, Fe and Ni elements are significantly reduced, the coating is mainly composed of Cr and N elements, the element content is stable, and the element content in the coating is higher than the element content in the substrate. The changing trend of the elements between the coating and the substrate is consistent with related research reports [32]. Figure 3(c) is a cross-sectional scan of the coating. The surface scan results are consistent with the line scan results, which indicates that nitrogen has successfully penetrated into the chromium coating to prepare a chromium nitrogen composite coating.

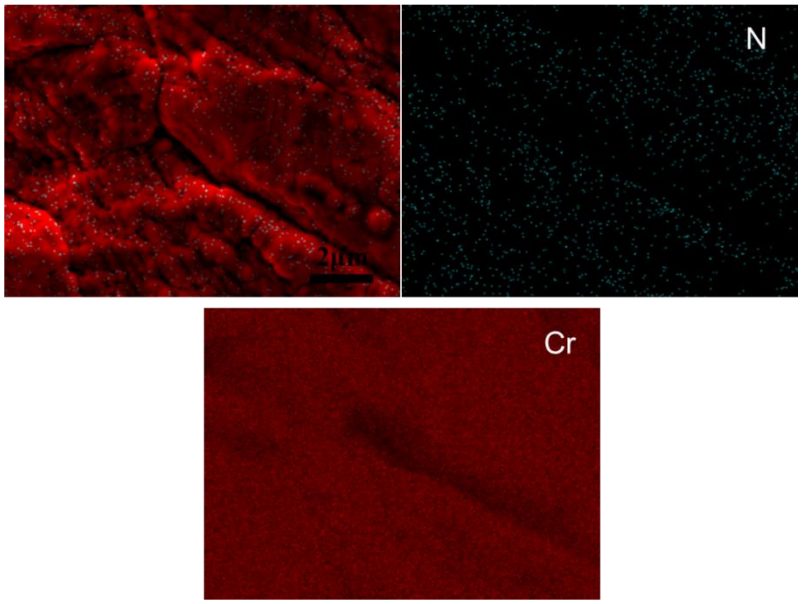

Figure 2. EDS surface analysis of Cr/N Composite Coating on etched 316 stainless steel surface

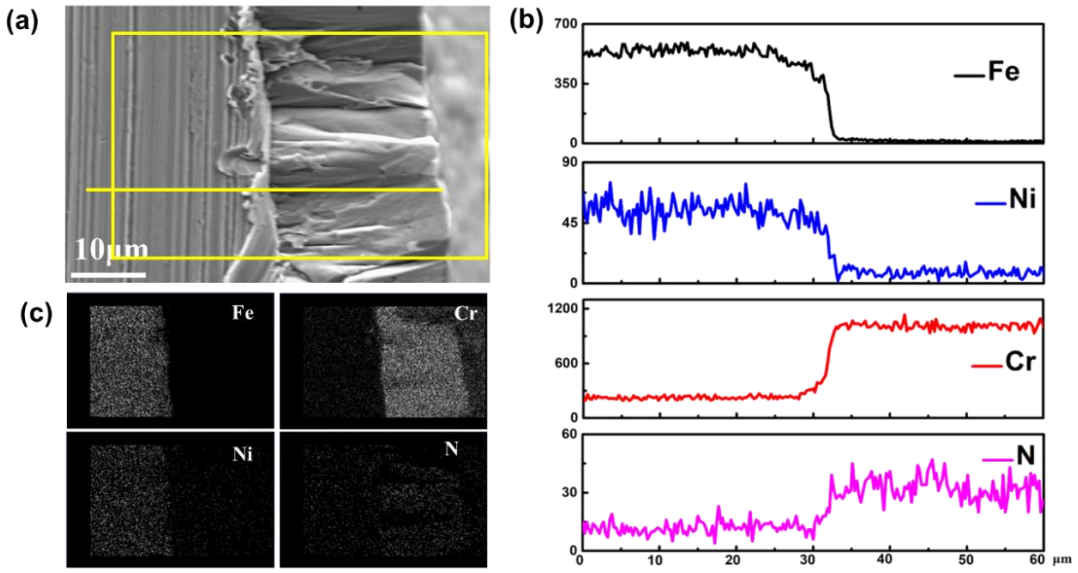

Figure 3. cross section of etched 316 stainless steel Cr/N Composite Coating: (a) cross section of etched 316 stainless steel Cr/N composite coating, (b) cross section of etched 316 stainless steel Cr/N composite coating, and (c) cross section of etched 316 stainless steel Cr/N composite coating

3.3. Structural analysis

Figure 4 shows the XRD diffraction pattern of the etched 316 stainless steel , chromium coating on etched 316 stainless steel and Chromium nitrogen composite coating on etched 316 stainless steel. It can be seen from the figure that 316 stainless steel is a typical crystalline structure. On the XRD diffraction pattern of chromium coating, there is an obvious amorphous steamed bun peak at the diffraction angle of about 43°[33], and the diffraction surface is (110), which is shown amorphous structure. In the XRD diffraction pattern of Chromium nitrogen composite coating, the (111) diffraction peak is added at the diffraction angle of about 36°, and it is still shown an amorphous structure. This means that no nitride is formed in the chromium coating after nitriding. During nitriding, the reaction voltage bombards the surface of the Cr coating, which provides an effective channel for the diffusion of N atoms, and promotes more N atoms to be uniformly distributed in the amorphous chromium coating in the form of solid solution through solid phase diffusion[34]. Meanwhile amorphous coatings are short-range ordered and long-term disordered, and there are no crystal defects such as grain boundaries, dislocations, and segregation, which is beneficial to improve the corrosion resistance of the coating.

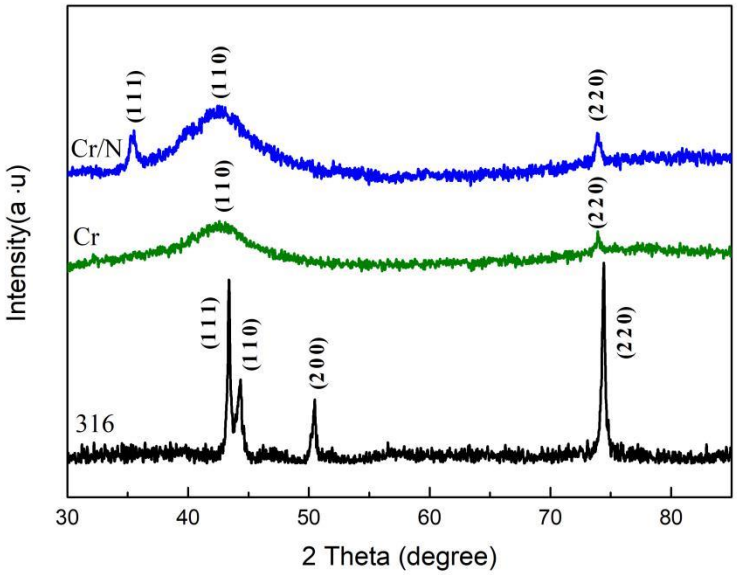

Figure 4. XRD patterns of etched 316 stainless steel, Cr coating and Cr/N composite coating

3.4. Corrosion resistance test

To verify the corrosion resistance of nitrited chromium composite coating, potentiodynamic polarization tests were carried out on 316 stainless steel and 316 stainless steel coated with nitrited chromium composite coating under the oxygen-enriched condition of 0.5 M H_2SO_4 + 5 ppm NaF, and the test results are shown in Figure 5. In the corrosion resistance test, the open circuit potential represents the corrosion trend, and the corrosion potential and current density are two important parameters to quantify the corrosion resistance of a material. Figure 5(a) shows the test results of open circuit potential. It can be seen from the figure that the open circuit potential of 316 stainless steel is obviously lower than

that of 316 stainless steel coated with nitrited chromium composite coating. A low open circuit potential means a higher corrosion tendency, which indicates that the plating 316 stainless steel with chromium-based nitride composite coating has good chemical stability in acidic environments. Figure 5(b) is the polarization curve of the blank 316 stainless steel and the 316 stainless steel plated with nitrited chromium composite coating. The polarization data is shown in Table 1. In this paper, the Tafel extrapolation method is used to obtain the corrosion potential density and corrosion potential from the slope intercept of the polarization curve [35,36]. The corrosion current density of 316 stainless steel is 1.1×10^{-4}A/cm^2, and the corrosion potential is -0.342V. The corresponding corrosion current density of 316 stainless steel plated with nitrited chromium composite coating is 9.35×10^{-7}A/cm^2, the corrosion potential is -0.212V, the corrosion potential shifts in the positive direction, and the corrosion current density is reduced by 3 orders of magnitude, which shows that Cr/N composite coating effectively improves the corrosion resistance of 316 stainless steel. The corresponding calculation formula of corrosion resistance efficiency (η_p) [37]:

$$\eta_p\ (\%) = \frac{i^0_{corr} - i_{corr}}{i^0_{corr}} \times 100$$

Among them, i^0_{corr} and i_{corr} are the corrosion current density of 316 stainless steel and 316 stainless steel with nitrited chromium composite coating, respectively. The corrosion efficiency of 99.15% further confirmed the excellent corrosion resistance of 316 stainless steel with nitrited chromium composite coating.

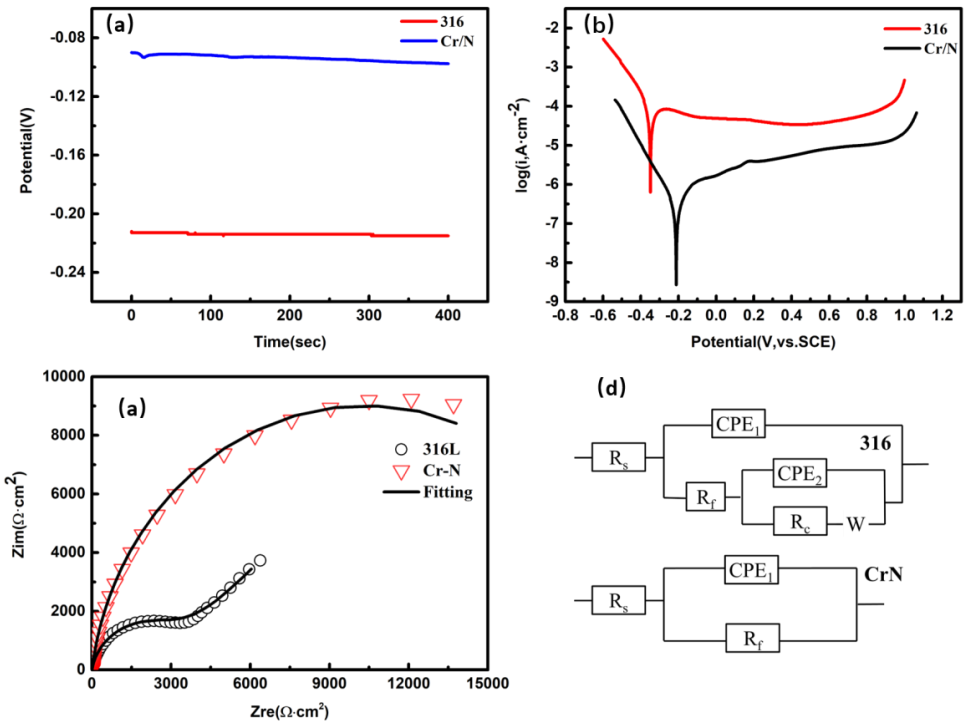

Figure 5. 0.5 M H_2SO_4+5ppm NaF oxygen rich 316 stainless steel and 316 stainless steel with Cr/N composite coating: (a)Open circuit potential, (b)polarization curve, (c) Nyquist, (d)equivalent circuit

The impedance test result is shown in Figure 5(c). It can be seen that the impedance arc diameter of the Cr/N composite coating is much larger than that of 316 stainless steel, indicating that the Cr/N composite coating is an effective anti-corrosion barrier. At the same time, the impedance diagram of 316 stainless steel consists of a semicircle in the high-frequency region and an upward tail in the low-frequency region. The diffusion tail of concentration polarization in the low-frequency region means that the corrosive liquid contacts the substrate after passing through the surface passivation film. The Cr/N composite coating has no diffusion arc, indicating that the corrosive solution does not pass through the coating to contact the substrate, indicating that the Cr/N composite coating is dense and effectively prevents the corrosive solution from contacting the substrate. Fit the corresponding equivalent circuit diagram according to the impedance result, as shown in figure 5(d). In the circuit diagram, R_s represents the solution resistance of the system, R_f represents the resistance of the stainless steel passivation film, R_c represents the charge transfer resistance of the stainless steel and the coating, CPE_1 represents the non-ideal passivation film capacitor, and CPE_2 represents the non-ideal electric double layer capacitor of stainless steel. W stands for Weber impedance. The fitting results are shown in Table 2. The charge transfer resistance of the Cr/N composite coating is as high as 20950 Ω·cm2, which is much higher than that of 316 stainless steel, indicating the excellent corrosion resistance of the Cr/N composite coating.

Table 1. electrochemical parameters of 316 stainless steel substrate and 316 stainless steel with Cr/N Composite Coating under oxygen enriched condition of 0.5 M H_2SO_4+5ppm NaF

Sample	**Icorr (A/cm^2)**	**Ecorr (V)**	**ηp (%)**
316	**1.1×10^{-4}**	**-0.342**	**-**
Cr/N	**9.35×10^{-7}**	**-0.212**	**99.15**

Table 2. equivalent circuit fitting electrochemical parameters of 316 stainless steel and 316 stainless steel with Cr/N Composite Coating under oxygen enriched condition of 0.5 M H_2SO_4 + 5 ppm NaF

Sample	Rs $\Omega\ cm^2$	CPE_1		Rf $\Omega\ cm^2$	CPE_2		Rc $\Omega\ cm^2$	Warburg Y0
		$Y0_1$ $\mu\Omega^{-1}\ cm^{-2}\ s^n$	n_1		$Y0_2$ $\mu\Omega^{-1}\ cm^{-2}\ s^n$	n_2		
316	2.736	1.07×10^{-4}	0.9035	1285	8.76×10^{-4}	0.7259	6380	1.00×10^{4}
Cr/N	2.343	4.08×10^{-4}	0.9089	-	-	-	20950	-

In order to verify the long-term corrosion resistance of the Cr/N coating, 316 stainless steel and 316 stainless steel plated with a nitrited chromium composite coating were immersed in 0.5 M H_2SO_4 + 5 ppm NaF solution under oxygen-rich conditions, and electrochemical tests were carried out. Figure 6

shows the open circuit potential and potentiodynamic polarization curves of 316 stainless steel and 316 stainless steel plated with a chromium-based nitride composite coating in 0.5 M H_2SO_4 + 5 ppm NaF solution for 1h, 3 days and 7 days. Table 3 shows the corresponding Polarization parameters. It can be seen from figure (a) that the open circuit potential of 316 stainless steel plated with Cr/N composite coating is much higher than that of the substrate.It can be seen from figure (b) and table 2 that long time immersion has little effect on Cr/N composite coating. After immersion, the corrosion potential of Cr/N composite coating is still very high, the corrosion current density is reduced by at least 2 orders of magnitude, and the corrosion resistance efficiency is more than 99.6%, indicating that Cr/N composite coating has long-term corrosion resistance.

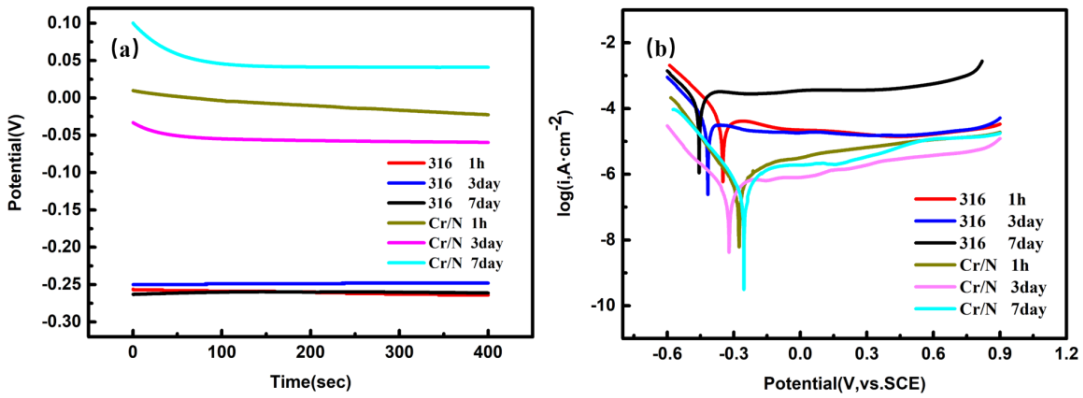

Figure 6. Comparison of immersion time of 316 stainless steel and 316 stainless steel with Cr/N Composite Coating in oxygen enriched condition of 0.5 M H_2SO_4 + 5 ppm NaF: (a)Open circuit potential,(b)polarization curve

Table 3. electrochemical parameters of 316 stainless steel and 316 stainless steel with Cr/N Composite Coating immersed in 0.5 M H_2SO_4 + 5 ppm NaF for different time

Soak time	Sample	Icorr (A/cm^2)	Ecorr (V)	η_p (%)
1h	**316**	8.128×10^{-5}	-0.349	-
	Cr/N	6.723×10^{-7}	-0.276	99.79
3day	**316**	7.44×10^{-5}	-0.393	-
	Cr/N	5.478×10^{-7}	-0.294	99.67
7day	**316**	3.8×10^{-4}	-0.456	-
	Cr/N	5.628×10^{-7}	-0.254	99.85

The Nyquist diagrams of 316 stainless steel and 316 stainless steel coated with Cr/N composite coating in 0.5 M H_2SO_4 + 5 ppm NaF solution under oxygen-enriched conditions for 1 hour, 3 days and 7 days are shown in Figure 7, and Table 4 is the corresponding fitting parameters. It can be seen that 316

stainless steel has a diffusion tail in the low frequency area, but as the immersion time increases, the radius of the arc gradually decreases, and the slope of the diffusion tail weakens or even disappears, indicating that 316 stainless steel does not have long-term corrosion resistance. The shape of the impedance diagram of the Cr/N composite coating after immersion is the same as that before the immersion, and the diameter of the arc of the Cr/N composite coating increases after long time immersion, indicating that the Cr/N composite coating has long, stable and efficient corrosion resistance.

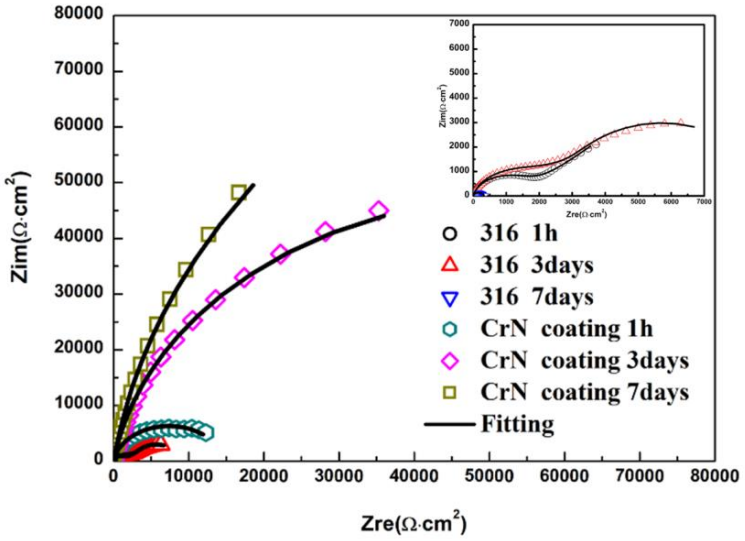

Figure 7. Nyquist diagram of 316 stainless steel and 316 stainless steel coated with Cr/N composite coating immersed in 0.5 M H_2SO_4 + 5 ppm NaF solution for a long time

Table 4. Fitting parameters of 316 stainless steel and 316 stainless steel with Cr/N Composite Coating immersed in 0.5 M H_2SO_4 + 5 ppm NaF solution for a long time

Soak time	Sample	Rs Ω cm²	CPE1		Rf Ω cm²	CPE2		Rc Ω cm²	Warburg Y0
			$Y0_1$ $\mu\Omega^{-1}$ cm^{-2} s^n	n1		Y02 $\mu\Omega^{-1}$ cm^{-2} s^n	n2		
1h	316	3.494	3.85×10^{-5}	1	36.94	7.58×10^{-5}	0.7898	3728	1.44×10^{-3}
	Cr/N	2.525	3.553×10^{-4}	0.9009	1473	4.387×10^{-4}	0.9986	16770	-
3day	316	2.353	8.75×10^{-5}	0.8871	96.87	3.99×10^{-5}	1.27×10^{-5}	5964	5.26×10^{-4}
	Cr/N	5.543	6.761×10^{-5}	1	86.42	1.027×10^{-4}	0.812	19430	-
7day	316	3.483	4.54×10^{-4}	0.8987	322.3	0.352	1	262	2.88×10^{7}
	Cr/N	1.913	1.556×10^{-4}	0.8205	26.96	4.34×10^{-5}	0.9011	224600	-

3.5. Conductivity test

The conductivity of Cr/N composite coatings was studied by interface contact resistance. The ICR values of 316 stainless steel and 316 stainless steel coated with Cr/N composite coatings under different pressures are shown in Figure 8. As the pressure increases, the ICR value decreases as the

effective contact area increases. In the entire test range, the ICR value of 316 stainless steel with Cr/N composite coating is lower than that of 316 stainless steel. When the contact pressure is 1.4MPa, the contact resistance of the Cr/N composite coating is 4.9mΩ·cm^2, which is lower than the US Department of Energy's requirement that the ICR value should be less than 10mΩ·cm^2. The low ICR of the coating indicates that the Cr/N composite coating effectively improves the conductivity of the bipolar plate, this phenomenon is consistent with the results of similar coating research reports [30,38].

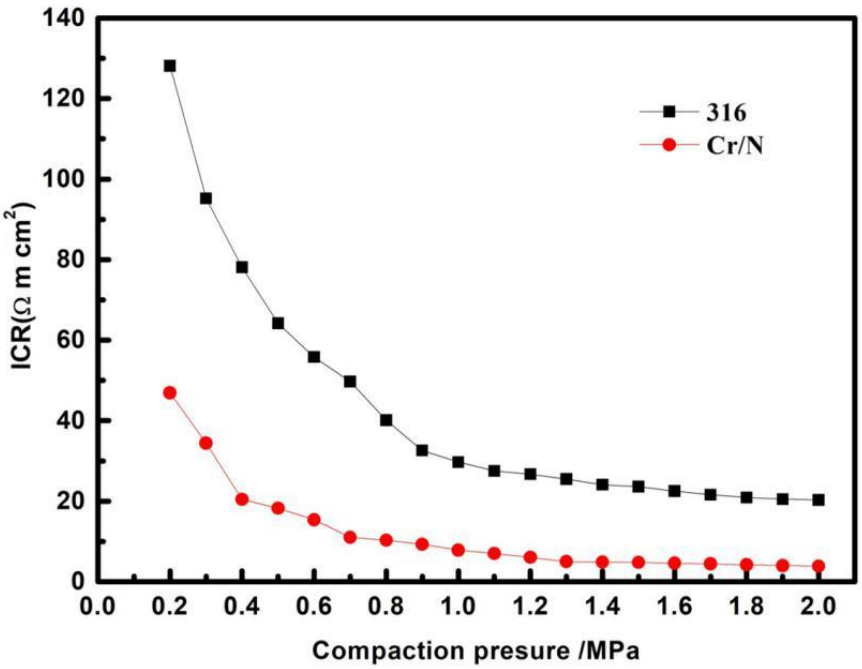

Figure 8. contact resistance curve of 316 stainless steel substrate and stainless steel with Cr/N Composite Coating

4. CONCLUSIONS

In this paper, Preparation of nitrited chromium composite coating on micro etched 316 stainless steel by a combination process of electrodeposition and liquid-phase plasma electrolysis. The coating with micro-nano structure shows obvious hydrophobicity, and the contact angle of the Cr/N composite coating is greater than 120°. Electrochemical analysis including Tafel curve and electrochemical impedance revealed that the Cr/N composite coating has excellent corrosion resistance. In the simulated PEMFC cathode environment, the corrosion current density of the Cr/N composite coating is 9.35×10^{-7}A/cm^2, which is 3 orders of magnitude lower than that of 316 stainless steel. Even the coating has been immersed for 1h, 3d, 7d, the corrosion current density of the coating is still in the range of 5.478×10^{-7} A/cm^2~6.723×10^{-7} A/cm^2. Meantime, the Cr/N composite coating also has low contact resistance. Under the contact pressure of 1.4MPa, the ICR value of the Cr/N composite coating is 4.9mΩ·cm^2, the contact resistance is one order of magnitude lower than that of the stainless steel substrate. The results show that

the Cr/N composite coating can be used as a promising protective coating for the stainless steel bipolar plate of the proton exchange membrane fuel cell.

ACKNOWLEDGEMENTS
This work was financially supported by National Natural Science Foundation of China (No. 21673135 and No. 21972090) and Science and Technology Commission of Shanghai Municipality (No. 17020500700, 18511110902 and 19DZ2271100).

References

1. J. Li, Z. Xu, Y. Li, X. Ma, J. Mo, L. Weng, C. Liu, *Journal of Materials Science*. 56 (2021) 8689-8703.
2. P. Yi, C. Dong, T. Zhang, K. Xiao, Y. Ji, J. Wu, X. Li, *Journal of Power Sources*. 418 (2019) 42-49.
3. H. Dong, S. He, X. Wang, C. Zhang, D. Sun, *Diamond and Related Materials*. 110 (2020).
4. X. Chen, Y. Chen, Q. Liu, J. Xu, Q. Liu, W. Li, Y. Zhang, Z. Wan, X. Wang, *Energy Reports*. 7 (2021) 336-347.
5. Y. Leng, P. Ming, D. Yang, C. Zhang, *Journal of Power Sources*. 451 (2020).
6. Z. Xu, D. Qiu, P. Yi, L. Peng, X. Lai, *Progress in Natural Science: Materials International*. 30 (2020) 815-824.
7. Z. Tu, H. Zhang, Z. Luo, J. Liu, Z. Wan, M. Pan, *Journal of Power Sources*. 222 (2013) 277-281.
8. N.J. Cooper, T. Smith, A.D. Santamaria, J.W. Park, *International Journal of Hydrogen Energy*. 41 (2016) 1213-1223.
9. K. Feng, Z. Li, H. Sun, L. Yu, X. Cai, Y. Wu, P.K. Chu, *Journal of Power Sources*. 222 (2013) 351-358.
10. M. Dadfar, M. Salehi, M.A. Golozar, S. Trasatti, *International Journal of Hydrogen Energy*. 41 (2016) 21375-21384.
11. R. Tian, J. Sun, L. Wang, *International Journal of Hydrogen Energy*. 31 (2006) 1874-1878.
12. J. Huang, D.G. Baird, J.E. McGrath, *Journal of Power Sources*. 150 (2005) 110-119.
13. J. Xuan, L. Xu, S. Bai, T. Zhao, Y. Xin, G. Zhang, L. Xue, L. Li, *International Journal of Hydrogen Energy*. 2021.04.119(2021).
14. Y. Fu, M. Hou, H. Xu, Z. Hou, P. Ming, Z. Shao, B. Yi, *Journal of Power Sources*. 182 (2008) 580-584.
15. E.A. Cho, U.S. Jeon, H.Y. Ha, S.A. Hong, *Journal of Power Sources*. 125 (2004) 178-182.
16. S. Pugal Mani, N. Rajendran, *Energy*. 133 (2017) 1050-1062.
17. X Z Yuan, H Wang, J Zhang, *Journal of New Materials for Electrochemical Systems*. 2005, 8(4): 257-267.
18. M. Li, S. Luo, C. Zeng, J. Shen, H. Lin, C.n. Cao, *Corrosion Science*. 46 (2004) 1369-1380.
19. S. Joseph, J. McClure, R. Chianelli, P. Pich, P. Sebastian, *International Journal of Hydrogen Energy*. 30 (2005) 1339-1344.
20. H. Wang, *Journal of Power Sources*. 115 (2003) 243-251.
21. S.H. Lee, N. Kakati, J. Maiti, S.H. Jee, D.J. Kalita, Y.S. Yoon, *Thin Solid Films*. 529 (2013) 374-379.
22. I.E. Paulauskas, M.P. Brady, H.M. Meyer, R.A. Buchanan, L.R. Walker, *Corrosion Science*. 48 (2006) 3157-3171.
23. J.H. Park, D. Byun, J.K. Lee, *Materials Chemistry and Physics*. 128 (2011) 39-43.
24. S. Joseph, J.C. McClure, P.J. Sebastian, J. Moreira, E. Valenzuela, *Journal of Power Sources*. 177

(2008) 161-166.
25. Y.H. Yun, *International Journal of Hydrogen Energy*. 35 (2010) 1713-1718.
26. S. Shimpalee, V. Lilavivat, H. McCrabb, Y. Khunatorn, H.K. Lee, *International Journal of Hydrogen Energy*. 41 (2016) 13688-13696.
27. Z. Qi, Z. Wu, D. Zhang, B. Wei, J. Wang, Z. Wang, *Vacuum*. 145 (2017) 136-143.
28. D. Zhang, L. Guo, L. Duan, W.-H. Tuan, *International Journal of Hydrogen Energy*. 36 (2011) 2184-2189.
29. O. Lavigne, C. Alemany-Dumont, B. Normand, S. Berthon-Fabry, R. Metkemeijer, *International Journal of Hydrogen Energy*. 37 (2012) 10789-10797.
30. E. Boztepe, A.C. Alves, E. Ariza, L.A. Rocha, N. Cansever, F. Toptan, *Surface and Coatings Technology*. 334 (2018) 116-123.
31. E. Haye, F. Deschamps, G. Caldarella, M.-L. Piedboeuf, A. Lafort, H. Cornil, J.-F. Colomer, J.-J. Pireaux, N. Job, *International Journal of Hydrogen Energy*. 45 (2020) 15358-15365.
32. D.-J. Shen, Y.-L. Wang, P. Nash, G.-Z. Xing, *Materials Science and Engineering*: A. 458 (2007) 240-243.
33. J. Huang, X. Fan, D. Xiong, J. Li, H. Zhu, M. Huang, *Surface and Coatings Technology*. 324 (2017) 463-470.
34. Z. Huang, Z.-X. Guo, L. Liu, Y.-Y. Guo, J. Chen, Z. Zhang, J.-L. Li, Y. Li, Y.-W. Zhou, Y.-S. Liang, *Surface and Coatings Technology*. 405 (2021).
35. J. Wu, K. Wang, L. Fan, L. Dong, J. Deng, D. Li, W. Xue, *Surface and Coatings Technology*. 313 (2017) 288-293.
36. C. E. Lu, N. W. Pu, K. H. Hou, C. C. Tseng, M. D. Ger, *Applied Surface Science*. 282 (2013) 544-551.
37. H. Shen, L. Wang, J. Sun, *Surface and Coatings Technology*. 385 (2020).
38. Y.Q. Hu, F. Chen, Z.D. Xiang, *Journal of Power Sources*. 414 (2019) 167-173.